



## Case study

## Failure analysis of the mobile elevating work platform



Srđan M. Bošnjak<sup>a,\*</sup>, Nebojša B. Gnjatović<sup>a</sup>, Dejan B. Momčilović<sup>b</sup>,  
Ivan L.J. Milenović<sup>a</sup>, Vlada M. Gašić<sup>b</sup>

<sup>a</sup> University of Belgrade, Faculty of Mechanical Engineering, Kraljice Marije 16, 11120 Belgrade, Serbia

<sup>b</sup> Institute for Testing of Materials IMS, Bulevar Vojvode Mišića 43, 11000 Belgrade, Serbia

## ARTICLE INFO

## Article history:

Received 28 September 2014

Received in revised form 14 March 2015

Accepted 16 March 2015

Available online 26 March 2015

## Keywords:

Mobile elevating work platform

Failure

Experimental investigations

Finite element analysis

## ABSTRACT

This paper presents an investigation of the accident which occurred during startup of the extending structure from the transport position. In order to clarify the causes of crack occurrence along almost the entire surface of the lever cross-section, the authors performed visual, experimental (chemical composition, tensile properties, microhardness) as well as metallographic examinations. Stress states in the critical zone are defined by applying the finite element method (FEM). Based on the investigation results it was concluded that the lever breakdown is predominantly caused by both the 'operating-in' defect (the malfunction of the limit switch) and the 'manufacturing-in' defect (poor weld quality). The investigation results presented in this paper are important because same or similar problems could arise in supporting structures of various types of transportation, construction and mining machines.

© 2015 Published by Elsevier Ltd. This is an open access article under the CC BY license (<http://creativecommons.org/licenses/by/4.0/>).

## 1. Introduction

The mobile elevating work platforms (MEWPs) are widely spread machines used for performing miscellaneous work at heights. During exploitation they are exposed to various loads, from deterministic to stochastic [1–3]. Despite the use of powerful design software [4] as well as new materials and technologies, accidents could not be avoided [5–7].

The extending structure of MEWP HP 13 is of a telescopic articulated type, Fig. 1. Failure of lever 3 occurred during startup of the extending structure from the transport position and at that along almost the entire surface of the cross-section in the vicinity of the end eye girder used for hydraulic cylinder connection, Fig. 2.

In order to identify the reasons behind the failure of lever 3, the following had to be performed:

- Visual examinations.
- An experimental procedure which, given the nature of the failure, includes: chemical composition analysis, tests of mechanical properties and microstructure examinations.
- Calculation of the stress state.

According to the design documentation, lever 3 was supposed to be made from steel quality grade S355JR [8] thickness of 4 mm.

\* Corresponding author. Tel.: +381 11 3370831; fax: +381 11 3370364.

E-mail address: [sbosnjak@mas.bg.ac.rs](mailto:sbosnjak@mas.bg.ac.rs) (S.M. Bošnjak).

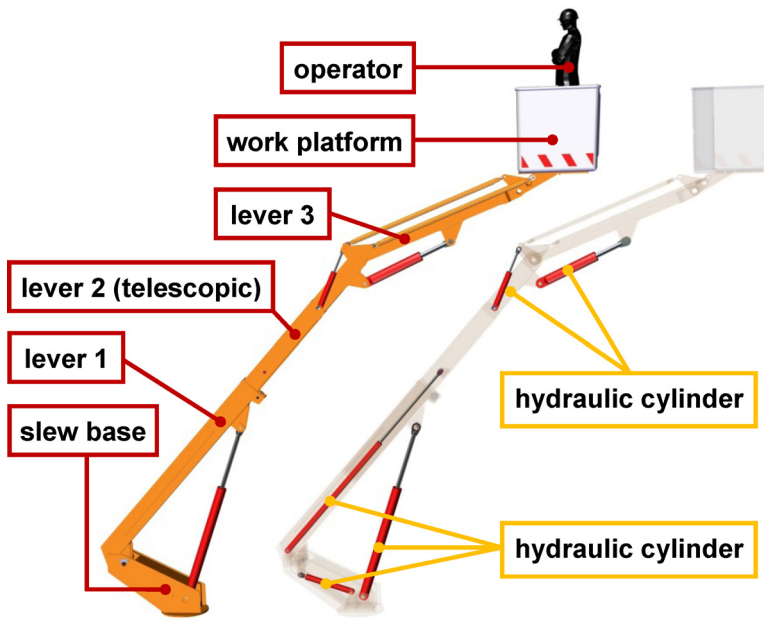


Fig. 1. Extending structure of the MEWP HP 13.

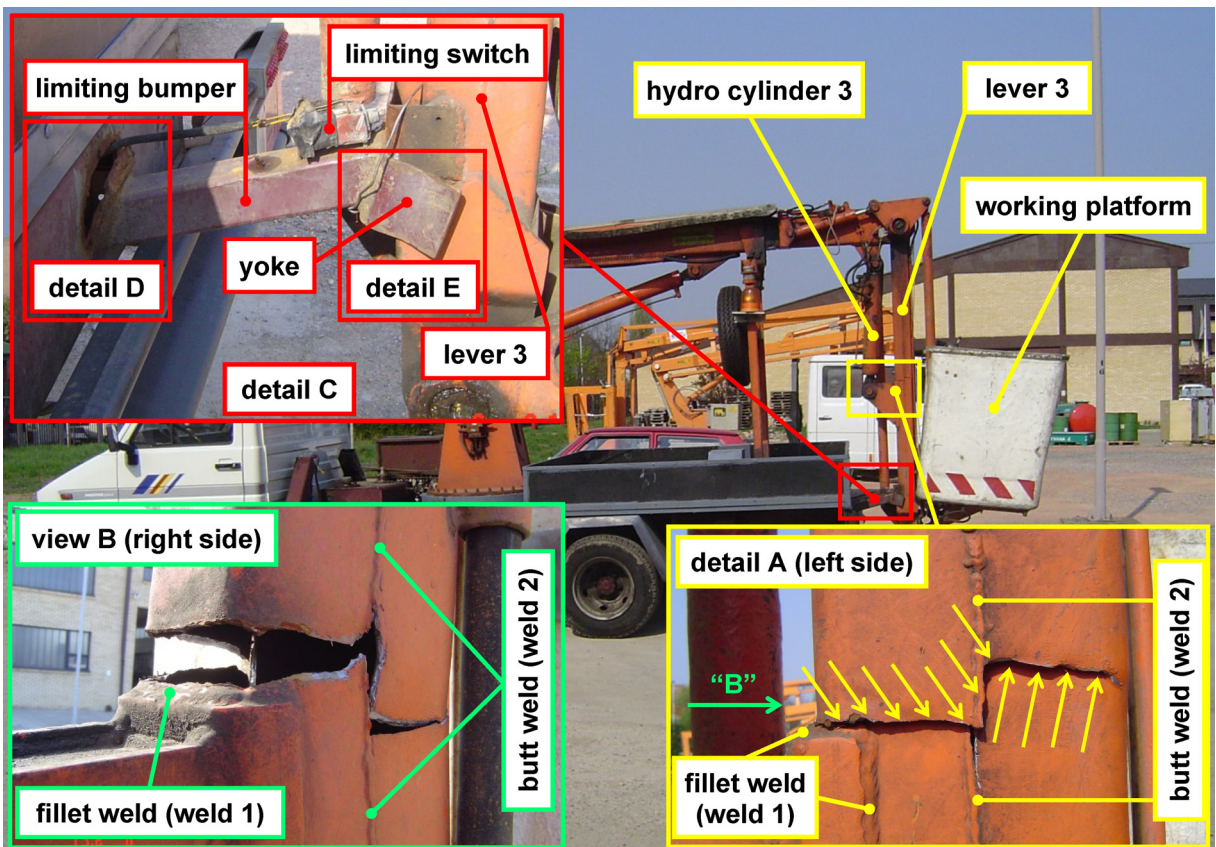


Fig. 2. Failure of lever 3.

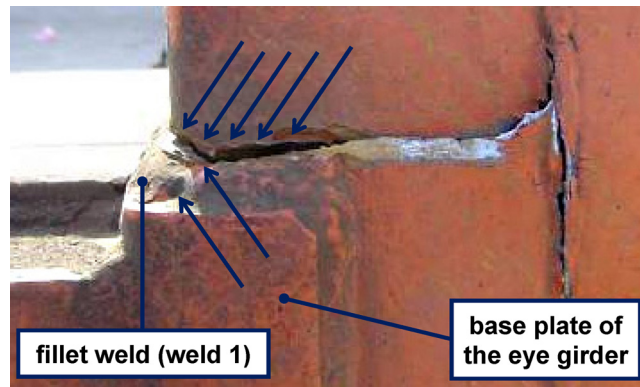


Fig. 3. Undercuts of weld 1.

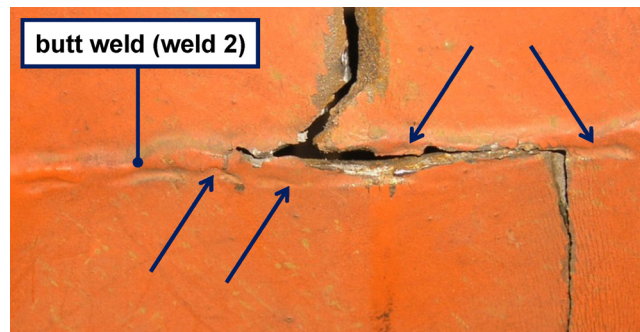


Fig. 4. Crack path vs. undercut zones of weld 2.

The investigation results presented in this paper are important because same or similar problems could arise in the supporting structures of various types of transportation, construction and mining machines. Besides that, they underline the importance of the position limiting devices for avoiding overloads of the structures with changeable geometry configuration.

## 2. Visual examinations

Visual examination [9] revealed that the thickness of weld metal 1, Fig. 2(detail A, view B) is from 2.5 to 5.5 mm which is different from the design requirements of 3 mm. The weld face shows spattering and irregular width of weld metal with partly continuous and partly intermittent undercuts along the full length of the weldment.

Generally, all weldments on the lever and eye girder, no matter what type (butt or filet) are made with unacceptable quality. Particularly dangerous are fillet welds with spotted continuous undercuts that connect the eye girder with the lever. The marked undercuts, Figs. 3 and 4, were significant stress raisers on the lever material with factor  $K_t$  higher than 3 [10]. Moreover, a closer look at the fracture zone reveals that the crack path follows the welding undercut zones, Fig. 4.

Two characteristic zones are observed on the crack surface, Fig. 5: zone 1 (detail A) cracked first, the conclusion based on obvious corrosion due to exposure to atmospheric conditions, and light zone 2 (detail B), light colored which indicates recent fracturing.

Plastic deformations of the limiting bumper yokes as well as failure of the welded connection between limiting bumper and auxiliary chassis were determined during visual examination, Fig. 2(detail C). Apart from that, observation disclosed that the limiting switch had suffered mechanical damage thus causing malfunction.

## 3. Experimental procedure

Due to the fact that the undamaged eye girder was mounted on the reconstructed lever 3, Fig. 6, all examinations were performed on specimens sampled from the damaged part of lever 3, Fig. 7.

Chemical analysis, Table 1, was conducted by the spectrometric method using the optical emission spectrometer ARL 360.

Tensile tests, Table 2, were carried out in a universal A.J. Amsler testing machine, according to the requirements of code [11].

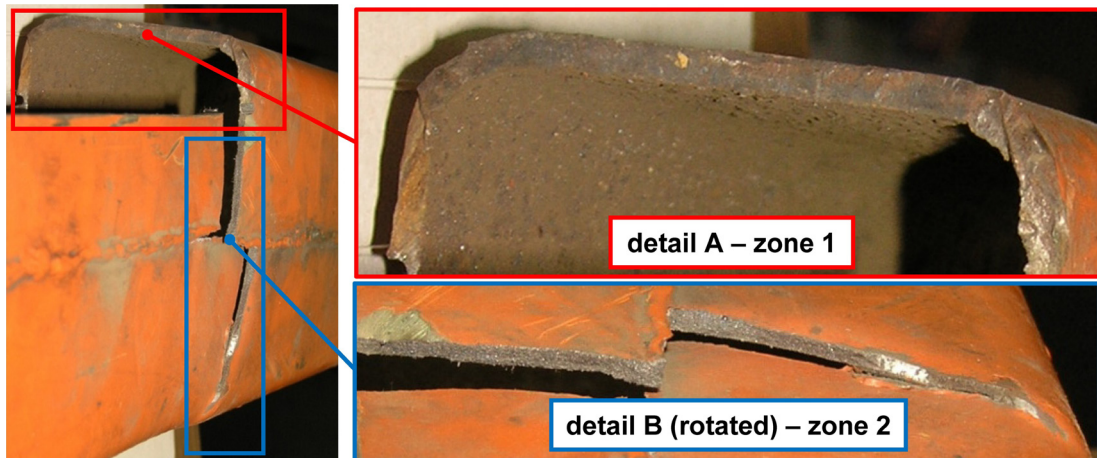


Fig. 5. Crack surface.

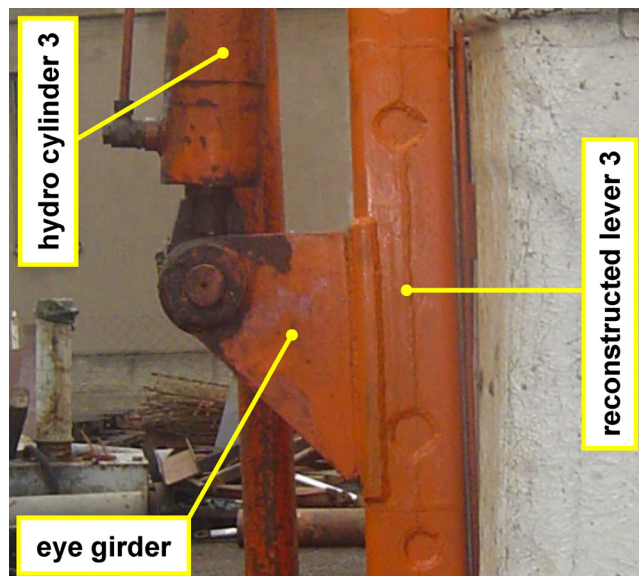


Fig. 6. Detail of the reconstructed lever 3.

The determination of hardness was carried out by microhardness (HV1) testing of specimens for metallographic examinations. The mentioned testing was performed as per [12] by means of the semiautomatic optical instrument HAUSER 249 A, Table 3.

A macro examination of the polished specimen revealed incomplete welding, an undercut and sagging, i.e. an incompletely filled groove, Fig. 8.

Microstructure examinations were made using the LM METAVAL, Figs. 9 and 10.

#### 4. Calculation of the stress state

The external load analysis is performed for the following two cases:

- Load case (LC) 1 – MEWP in normal operation. According to the code [3] the following loads are taken into account: the rated load, structural loads, wind loads and manual forces.
- LC 2 – lever 3 is leaning against the limiting bumper. Besides the rated and structural loads, lever 3 is also exposed to the maximum retraction force (86.2 kN) of the hydraulic cylinder 3, which is the consequence of the malfunction of the limit switch (see Section 2) used for deactivation of the hydraulic system once lever 3 reaches the transportation position.



Fig. 7. Part of the damaged lever 3 used for sampling.

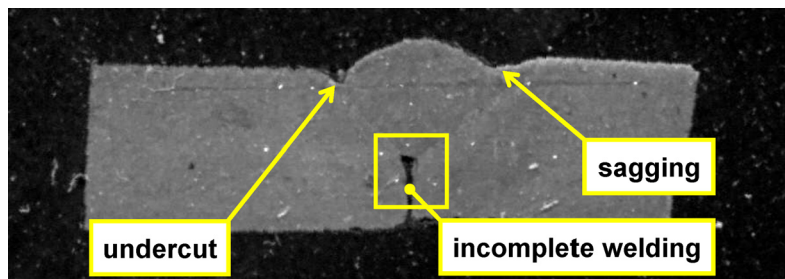


Fig. 8. Multiple weld defects of weld 2.

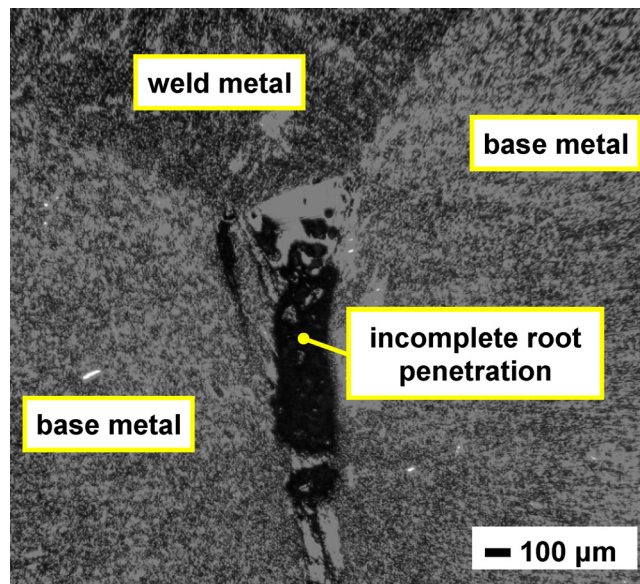


Fig. 9. Micrograph of the incomplete root fusion (squared detail shown in Fig. 8).

The identification of the stress state is done by applying the linear finite element method (LFEM). In LC 1 for the complete working envelope of lever 3, Fig. 11a, the maximum von Mises stress values in the zone of crack occurrence do not exceed  $\sigma_{vM,max}^{LC1} = 108$  MPa, Fig. 11b. That value is obtained when the hydraulic cylinder 3 is completely extended, Fig. 11c, i.e. for  $\alpha = \alpha_{max} = 95^\circ$ . For LC 2 the maximum von Mises stress value in the critical zone is  $\sigma_{vM,max}^{LC2} = 418$  MPa, Fig. 12.

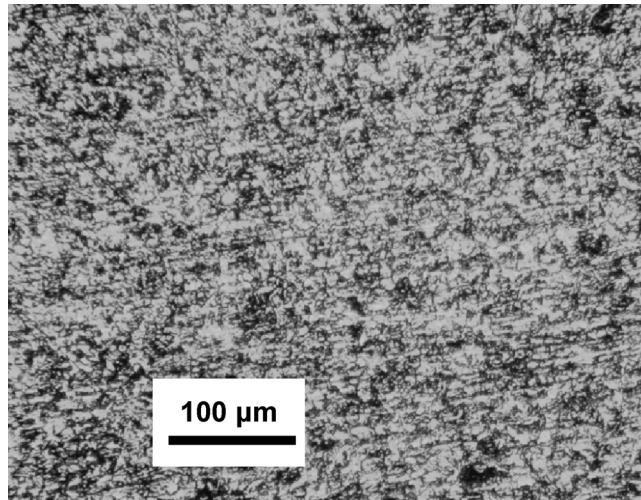


Fig. 10. Ferrite–pearlite microstructure of the base metal (common for general structure steel).

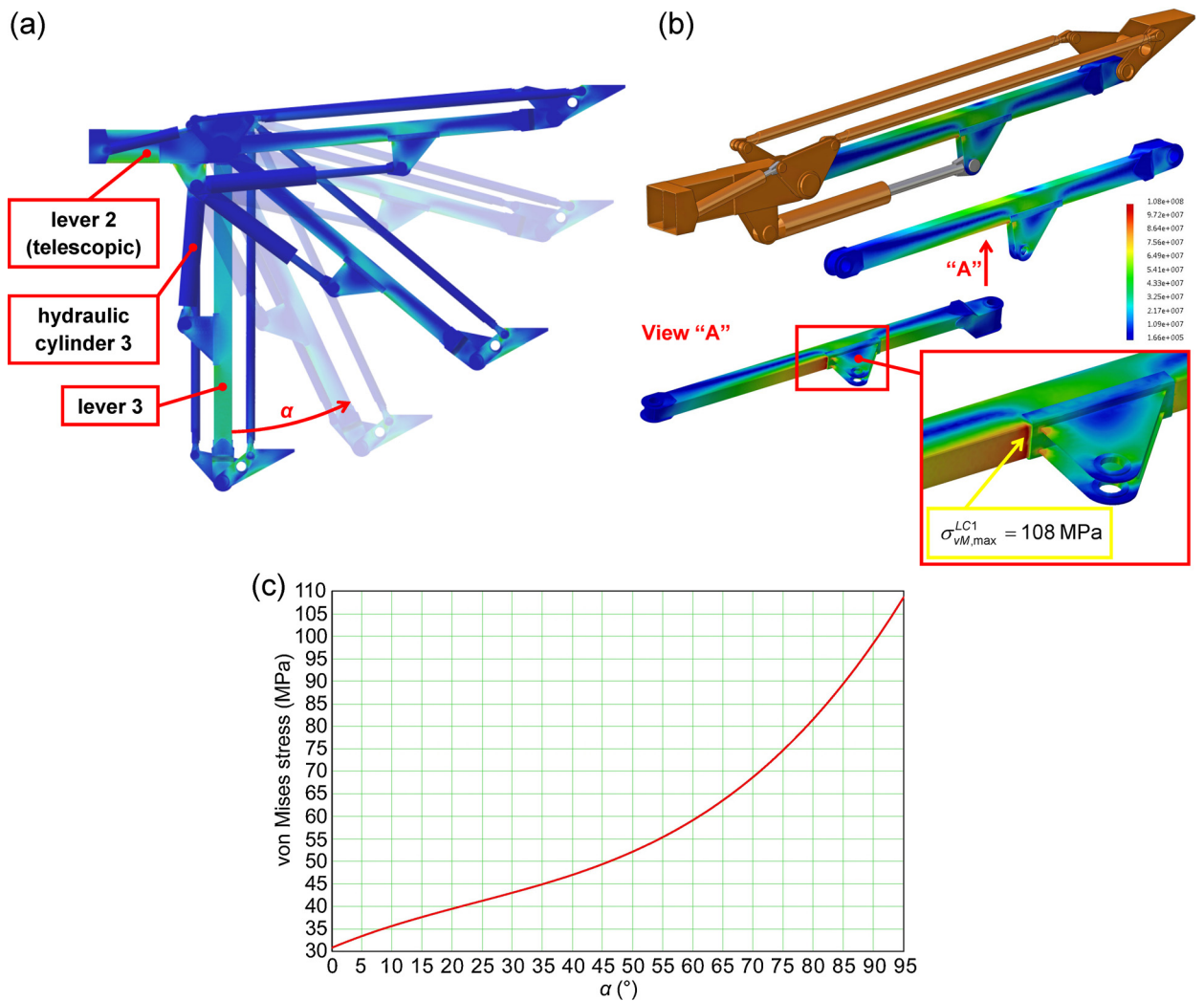


Fig. 11. von Mises stress state of level 3 in LC 1: (a) working envelope ( $\alpha_{min} = 0^\circ$ ,  $\alpha_{max} = 95^\circ$ ); (b) stress field for  $\alpha_{max}$ ; (c) dependence of the maximum von Mises stress in the critical zone on the angle between level 2 and level 3.

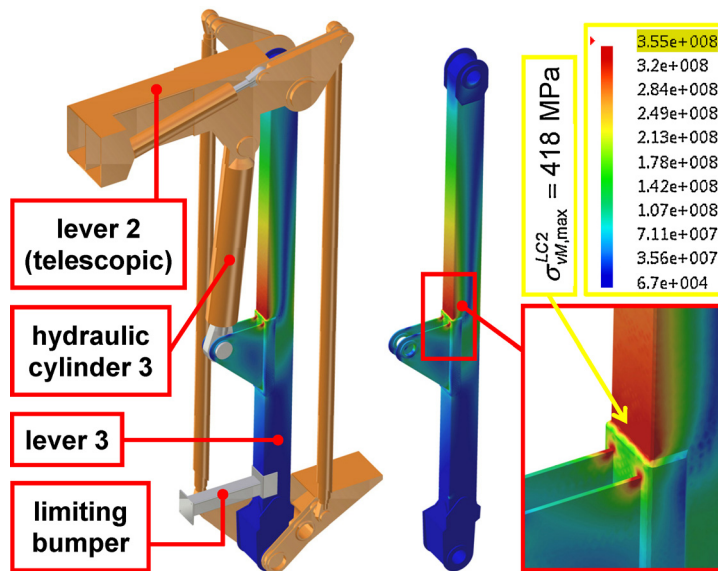


Fig. 12. Von Mises stress state of lever 3 in LC 2.

Table 1

Chemical analysis (wt.%) of lever 3 material and chemical composition of S355JR [8].

Material	C	Si	S	P	Mn
Specimen S355JR	0.156 max. 0.24	0.174 max. 0.55	0.019 max. 0.035	0.15 max. 0.035	1.408 max. 1.6

Table 2

Tension test [11] results and tensile properties of S355JR [8].

Material	$\sigma_{ys}$ (MPa)	$\sigma_{UTS}$ (MPa)	Elongation $A_5$ (%)
Specimen 1	389	539	28.2
Specimen 2	380	534	28.2
Specimen 3	369	531	30.0
S355JR	min. 355	470–630	min. 22

Table 3

Microhardness test [12] results.

Location	Microhardness (HV1)
Base metal	182 – 178 – 182
Heat affected zone	210 – 257 – 223 – 253
Weld metal	240 – 234 – 229

## 5. Conclusion

Conclusions arrived at herein are based on the results presented in Sections 2–4 and are listed below:

- The lever 3 material meets the requirements of code [8] defined for steel grade S355JR, Tables 1–3.
- Poor manufacturing practice led to multiple welding defects on the base plate of the eye girder (weld 1), Figs. 2 and 3. Such defects significantly accelerate premature crack initiation by playing a role, from the welding point of view, as the local HAZ based weak link, as shown in Figs. 8 and 9. The paper [10] shows that the magnitude of stress considerably increases in the presence of welding defects.
- Butt welds on lever 3 have many defects, such as incomplete welding, the undercut and sagging, Figs. 8 and 9.
- The location of the maximum calculated stress values corresponds to the crack location, Figs. 2, 11 and 12.

- The calculated stress value in the critical zone for LC 2 ( $\sigma_{vM,max}^{LC2} = 418$  MPa, Fig. 12) is higher for 7.5% than the maximum yield stress value obtained by testing ( $\sigma_{YS} = 389$  MPa, Table 2). Furthermore, the finite element model does not include unfavorable influence of the welding defects observed during visual examinations (Section 2), which substantially, more than three times [10], multiplies the local level of stress states. Accordingly, we can conclude that even for intensities of the retraction force of the hydraulic cylinder 3 that are lower than its maximum value, stress values higher than the ultimate tension stress values (obtained by testing, Table 2) are certain to appear.
- The overload caused by the effect of the retraction force of the hydraulic cylinder 3 (LC2) is unambiguously testified by the appearance of plastic deformations of the limiting bumper yokes, Fig. 2 (detail C).
- The results of visual examination lead to the conclusion that initial cracking occurred in HAZ in close vicinity of the undercuts (zone 1, Fig. 5, detail A), due to the overload as a result of the limiting switch failure. The propagation of the crack, due to repeated overloads, led to final failure by cracking of lever 3 near the eye girder (zone 2, Fig. 5, detail B).

The presented results of the numerical-experimental analyses led to the conclusion that the main causes of the extending structure breakdown were:

- Malfunction of the limit switch ('operating-in' defect [13,14]) which caused the unforeseen loading, not predicted by the project documentation.
- Poor weld quality [15] ('manufacturing-in' defect [13]).

### Acknowledgment

This work is a contribution to the Ministry of Education, Science and Technological Development of Serbia funded project TR 35006.

### References

- [1] Bošnjak S, Zrnić N, Dragović B. Dynamic response of mobile elevating work platform under wind excitation. *Stroj Vestn-J Mech Eng* 2009;55(2): 104–113.
- [2] Bošnjak S, Zrnić N, Gašić V, Petković Z, Milovančević M. Dynamic responses of mobile elevating work platform and mega container crane structures. *Adv Mater Res* 2012;562–564:1539–43.
- [3] EN 280. Mobile Elevating Work Platforms – Design Calculations – Stability Criteria – Construction – Safety – Examinations and Tests. European Committee for Standardization; 2009.
- [4] Derlukiewicz D, Przybyłek G. Chosen aspects of FEM strength analysis of telescopic jib mounted on mobile platform. *Automat Constr* 2008;17:278–83.
- [5] Pan C, Hoskin A, McCann M, Lin ML, Fearn K, Keane P. Aerial lift fall injuries: a surveillance and evaluation approach for targeting prevention activities. *J Safety Res* 2007;38:617–25.
- [6] Toribio J, Kharin V, Ayaso FJ, González B, Matos JC, Vergara D, Lorenzo M. Failure analysis of a lifting platform for tree pruning. *Eng Fail Anal* 2010;17:739–47.
- [7] Smith T. An evaluation of fatigue cracking in an aerial platform yoke from a fire-fighting vehicle. *Eng Fail Anal* 2002;9:303–12.
- [8] EN 10025-2. Hot Rolled Products of Structural Steels – Part 2: Technical Delivery Conditions for Non-alloy Structural Steels. European Committee for Standardization; 2004.
- [9] Brooks RC. Metallurgical Failure Analysis. New York: McGraw-Hill; 1993.
- [10] Cerit M, Kokumer O, Genel K. Stress concentration effects of undercut defect and reinforcement metal in butt welded joint. *Eng Fail Anal* 2010;17: 571–578.
- [11] EN 10002-1. Metallic Materials – Tensile Testing – Part 1: Method of Test at Ambient Temperature. European Committee for Standardization; 1990.
- [12] ISO 4516. Metallic and related coatings – Vickers and Knoop microhardness tests. Int Organ Stand 1980.
- [13] Gagg CR. Failure of components and products by 'engineered-in' defects: Case studies. *Eng Fail Anal* 2005;12:1000–26.
- [14] Bošnjak S, Arsić M, Zrnić N, Rakin M, Pantelić M. Bucket wheel excavator: integrity assessment of the bucket wheel boom tie-rod welded joint. *Eng Fail Anal* 2011;18:212–22.
- [15] EN ISO 5817. Fusion-welded Joints in Steel, Nickel, Titanium and their Alloys (Beam Welding Excluded) – Quality Levels for Imperfections. European Committee for Standardization; 2012.